



Trans. Nonferrous Met. Soc. China 31(2021) 1939–1950

Transactions of Nonferrous Metals Society of China

www.tnmsc.cn



### Isothermal extrusion speed curve design for porthole die of hollow aluminium profile based on PID algorithm and finite element simulations

Jie YI<sup>1</sup>, Zhi-wen LIU<sup>2</sup>, Wen-qi ZENG<sup>1</sup>

- 1. School of Mechanical Engineering, Hunan Industry Polytechnic, Changsha 410208, China;
- 2. School of Mechanical Engineering, University of South China, Hengyang 421001, China

Received 30 July 2020; accepted 24 December 2020

**Abstract:** The isothermal extrusion process of hollow aluminium profile was investigated using incremental proportional–integral–derivative (PID) control algorithm and finite element simulations. The range of extrusion speed was determined by considering the maximum extrusion load and production efficiency. By taking the optimal solution temperature of the secondary phase as the target temperature, the extrusion speed–stroke curve for realizing the isothermal extrusion of the aluminium profile was obtained. Results show that in the traditional constant extrusion speed process, the average temperature of the cross-section of the aluminium profile at the die exit rapidly increases and then slowly rises with the increase in ram displacement. As the extrusion speed increases, the temperature difference at the die exit of the profile along the extrusion direction increases. The exit temperature difference between the front and back ends of the extrudate along the extrusion direction obtained by adopting isothermal extrusion is about 6.9 °C. Furthermore, the heat generated by plastic deformation and friction during extrusion is balanced with the heat transfer from the workpiece to the container, porthole die and external environment.

Key words: isothermal control; extrusion speed curve; porthole die extrusion; PID control; heat balance

#### 1 Introduction

The use of lightweight materials is effective in energy and reducing conserving emission. Aluminium alloy is an ideal material for automobile lightweight components due to its advantages, such as low density, high specific strength, high specific stiffness and good crashworthiness [1-5]. An aluminium space frame car body possesses low mass, high stiffness and good collision performance and is therefore widely used by automobile manufacturers [6]. Extrusion profile is the main structural form of aluminium alloy applied in aluminium space frame car bodies. Compared with a steel body structure, the forming process of aluminium profiles is immature and costly. The production efficiency is increased using constant

extrusion speed in the industrial extrusion of aluminium profiles [7,8]. The extrusion exit temperature is a key factor in determining the quality of extrusion profiles. In the traditional extrusion process, the temperature of extrudate at the die exit gradually rises along the extrusion direction due to various comprehensive factors, including plastic deformation heat, frictional heat, heat transfer among billet and extrusion tools, which affect the uniformity of the microstructure and the mechanical properties of aluminium profiles [9-11]. Therefore, the traditional extrusion process that uses constant extrusion speed cannot meet the requirements of the high-performance of an aluminium profile. Isothermal extrusion refers to an extrusion process during which the temperature of profile at the die exit remains constant [12–14], and the deformation resistance and flow behaviour

of the material in the deformation zone of the die orifice remain uniform.

Many factors affect the temperature of the extrudate at the die exit, including extrusion speed, billet temperature, heating temperature of extrusion tools and die structures [15-17]. Isothermal extrusion can be achieved through numerous ways. One of these methods is the gradient heating of billet, in which a billet is formed at a certain temperature gradient along the axial direction by gradient heating or gradient cooling after uniform heating [18,19]. The excess heat generated by plastic deformation and friction is absorbed by the low-temperature part at the back end of the billet, so that the temperatures of the deformation zone and extrusion exit remain constant throughout the extrusion process. JENISTA [20] introduced a cooling system that can achieve the required temperature gradient of a billet. LI et al [21] developed a finite difference model to predict the transient temperature field of an aluminium billet in the gradient cooling process. However, accurately determining the billet temperature gradient through theoretical analysis in practical application is difficult, and using a special heating or cooling equipment increases the cost of extrudate production. The second method is regulating the extrusion speed through the on-line measurement of the extrusion exit temperature [22]. The extrusion exit temperature is fed back to the programmable logic controller of the extruder in real time, and the extrusion speed is subsequently adjusted accordance with the difference between measured and ideal exit temperatures to maintain constant exit temperature. PANDIT MÜLLER [23] used an infrared thermometer to measure the extrusion exit temperature and established a set of isothermal extrusion control systems. The efficiency of extrudate production was improved by 23% compared with the efficiency of the traditional extrusion process, and the product quality increased. However, this method has several disadvantages, such as lag of adjustment and inaccuracy of temperature measurement and control. The third method is the variable speed extrusion process [24]. In this method, the extrusion process is simulated through finite element (FE) techniques. The curve of the extrusion speed decreases with the increase in ram displacement, and thus enables the achievement of isothermal extrusion. The required

extrusion speed-stroke curve for isothermal extrusion is obtained in a computer simulation environment and then directly inputted into the PCL system of the extruder implementation of isothermal extrusion. YANG et al [25] proposed a basic method for realizing the isothermal extrusion of a large-size aluminium tube with piece wing. A new exit temperature versus ram displacement diagram was obtained through 3D FE method simulations at five different speeds. LI and LOU [26] developed a simulation model based on the principle of PID control to establish ram speed profiles that can suppress the temperature evolution during the extrusion process to obtain isothermal extrusion. ZHOU et al [27] derived two ram speed profiles from the simulation results of a series of conventional extrusion runs to maintain the workpiece maximum temperature of 7075 aluminium profiles at approximately 500 and 480 °C, respectively. Variable speed extrusion is an ideal method for realizing isothermal extrusion. The prediction of extrusion exit temperature is the key to realize isothermal extrusion. FE simulation is a scientific and effective means for optimizing the forming process, die structure and predicting the extrusion exit temperature [28-30]. However, the accurate control of the exit temperatures of complex hollow profiles through variable speed extrusion has not been yet reported. The Lagrange transient algorithm cannot solve the problem of self-contact in the welding of dividing extrusion metals in welding chamber for complex cross-section profile. In the arbitrary Lagrangian-Eulerian algorithm, the FE meshes are fixed in space, and mesh distortion and frequent remeshing are avoided [31-33]. Therefore, in this study this algorithm was used to simulate the transient extrusion process of a complex hollow profile.

The problem regarding the uniform exit temperature of hollow aluminium profile along the extrusion direction was solved by using the transient arbitrary Lagrangian—Eulerian method to calculate the temperature distribution of profile at the die exit under different extrusion speeds. The range of extrusion speed was determined by considering the maximum extrusion load and production efficiency. The optimal solution temperature of the secondary phase was used as the target temperature, and the extrusion speed—stroke curve for realizing the isothermal extrusion of

aluminium profiles was obtained using PID control algorithm FE incremental simulations. The accuracy and reliability of isothermal extrusion were verified with industrial non-contact infrared thermometer, which was used to monitor and record the temperature distribution of the die exit.

#### 2 Hollow profile and porthole die

An aluminium alloy anti-collision beam for automobile body was used in this study. The cross-sectional structure and dimension diagram are shown in Fig. 1. The profile was manufactured using 6063 aluminium alloy. The maximum and middle wall thickness values were 3 and 2.5 mm, respectively. The billet was difficult to extrude at a uniform metal flow velocity at die exit for this profile. The extrusion experiments and production of profile were conducted on an 1800 t horizontal extruder. The diameter of the extrusion container was 185 mm, and the extrusion ratio was 20. The porthole die included upper and lower dies. Four portholes were symmetrically arranged on the die surface to achieve uniform material flow. Two baffle plates were added at the left and right ends of the die orifice. The designed porthole die is shown in Fig. 2.

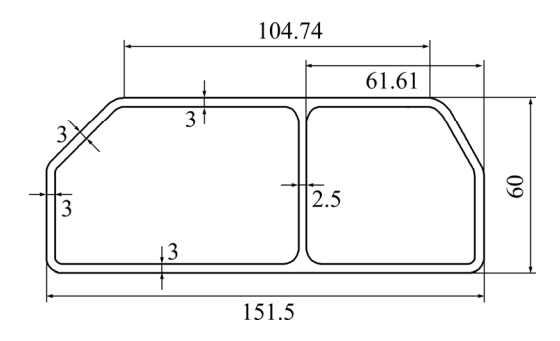
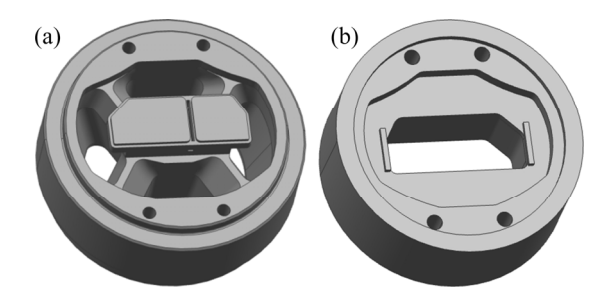


Fig. 1 Sectional shape and sizes of profile (unit: mm)



**Fig. 2** Porthole dies for manufactuing aluminium profile: (a) Upper die; (b) Lower die

# 3 FE modelling of transient extrusion process by using porthole die

The transient extrusion processes of simple hollow profiles are generally simulated using the arbitrary Lagrange algorithm based on mesh adaptive updating function. However, this algorithm cannot be used to analyze the welding self-contact problem of unsymmetrical complex profiles. To improve the simulation accuracy and reduce the simulation time, the transient arbitrary Lagrangian-Eulerian method with fixed elements was adopted to analyze the isothermal extrusion processes of the profiles (i.e. the initial states of the calculation elements were always conserved during the entire simulation process). The entire extrusion simulation process was divided into 35 steps. The purpose of the first five steps was to accelerate the extrusion ram, whereas the remaining 30 steps were the stages of the material extruded throughout the porthole die.

#### 3.1 FE mesh model

The FE model for simulating the porthole die extrusion process of a profile was established using the HyperMesh software (Fig. 3). The efficiency of element generation and the quality of the element were improved by dividing the entire model into several continuous regions, namely, billet, porthole, welding chamber, bearing and free-surface. For the transient-state analysis, the length of the free surface of the extruded profile was three times that of the die bearing, and that of the billet was two times the inner diameter of the container. The mesh continuity of different components was ensured by using a setup where the basic principle of mesh generation was from small to large and the meshing order was bearing  $\rightarrow$  welding chamber  $\rightarrow$ porthole → billet. To improve the accuracy and speed of simulation, a pentahedral mesh was used for the free surface and bearing, whereas a tetrahedral mesh was utilized for the billet, porthole and welding chamber. At least four free nodes were present at the thinnest section of the profile. The element size was not larger than 1/5 of the thinnest size of the profile and the length/width ratio of the pentahedral mesh for the die bearing was lower than 3. In general, the element size of the welding chamber was 2.5 times that of the bearing, the

element size of porthole was three times that of the welding chamber and the element size of the billet was three times that of the porthole.

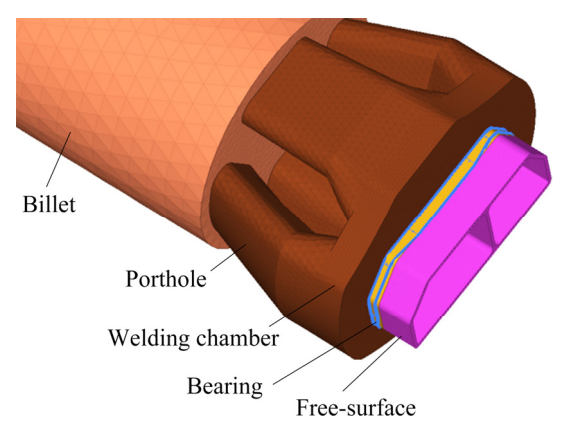


**Fig. 3** Mesh generation of finite element model for billet material

#### 3.2 Constitutive model of hot-deformed material

In the numerical simulation of the aluminium alloy extrusion process, a material is usually assumed as an incompressible viscoplastic non-Newtonian fluid. Considering the fact that thermal activation occurs in a high-temperature creep process, SELLARS and TEGART [34] proposed a hyperbolic sinusoidal flow stress function that includes the deformation activation energy and temperature and introduced an Arrhenius relationship to describe the thermal activation behaviour. The material constitutive equation is expressed as

$$\overline{\sigma} = \frac{1}{\beta} \sinh^{-1} \left\{ \frac{\dot{\varepsilon}}{A_{l}} \exp[Q/(RT)] \right\}^{1/n}$$
 (1)

where  $\bar{\sigma}$  is the flow stress of the material;  $\dot{\varepsilon}$  is the strain rate;  $A_1$ ,  $\beta$  and n are the temperature independent constants; R is the mole gas constant, 8.314 J/(mol·K); T is the thermodynamic temperature; Q is the deformation activation energy, which reflects the equilibrium relationship between strain hardening and dynamic softening during high-temperature plastic deformation.

In practical application, the flow stress value of the material under any deformation condition can be obtained if the material constants ( $A_1$ , Q,  $\beta$  and n) are known. The constitutive model parameters of a 6063 aluminium alloy are as follows [35]:  $A_1$ =5.91×10<sup>9</sup> s<sup>-1</sup>; Q=1.415×10<sup>5</sup> J/mol;  $\beta$ =4×10<sup>-2</sup> m<sup>2</sup>/MN; n=5.385.

#### 3.3 Frictional and thermal boundary conditions

In addition to the material constitutive model, the frictional and thermal boundary conditions of each contact interface (Fig. 4) are important factors that affect the simulation accuracy. These parameters are difficult to measure directly through experiments. A Coulomb or shear friction model is generally used in the numerical simulation of an extrusion. The friction coefficient is obtained using a table or by experience, and thus cannot reflect the friction behaviour of the contact interface. Accurate simulation results can be obtained by using frictional boundary conditions that are close to the actual values in the simulation. In addition, the established friction model should reflect the friction physical nature of a workpiece/die interface. In the extrusion process, the friction amongst the extrusion cylinder, die and material is adhesive friction, and the friction coefficient is set to be 1 to achieve an acceptable FE simulation accuracy. The friction behaviour in die bearing is complex, and the full adhesion friction in the inlet gradually transits to sliding friction in the outlet of the die bearings. Therefore, a shear-type friction was defined. Through the secondary development of the tool command language in the HyperXtrude software, the friction stress per unit area was inputted into the boundary conditions of the simulation software (Fig. 5). In the extrusion process, the heat transfer amongst the material, die and external environment has an important effect on the material flow and extrusion temperature. The heat transfer coefficients of the interface amongst the container, die and material and between the extruded profile and the external environment were 3000 and 20 W/(m<sup>2</sup>.°C), respectively. Table 1 shows the detailed contact boundary conditions in the FE simulation model.

In this study, 6063 material was used for an extrusion billet. The preheating temperatures of the

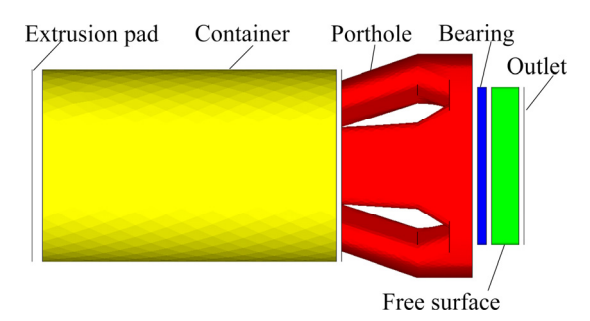


**Fig. 4** Contact interface of different parts of material in extrusion process of profile porthole die

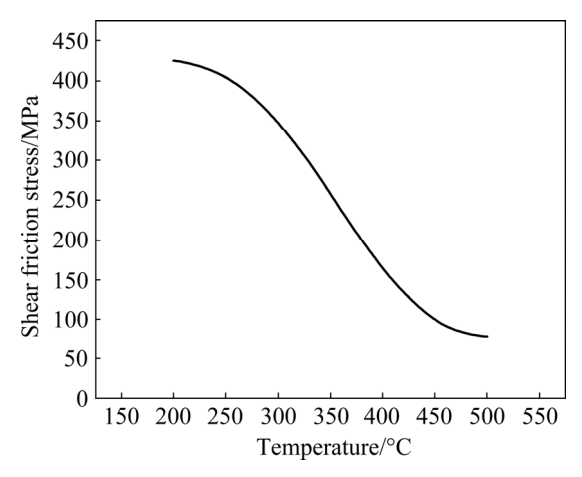


Fig. 5 Variation of steady shear friction stress with temperature

extrusion cylinder and porthole die were 430 and 480 °C, respectively, the heating temperature of the billet was 480 °C and the extrusion ratio was 20. The specific process parameters are summarized in Table 2.

# 4 Simulated isothermal extrusion process based on PID control method

The digital PID control algorithm includes positional and incremental PID control ones [36]. In this study, the incremental digital PID algorithm was used in the analogue control process. The calculation formula is written as follows:

 $\Delta u(k) = Ae(k) - Be(k-1) + Ce(k-2) \tag{2}$ 

where  $A=K_P+K_I+K_D$ ,  $B=K_P+2K_D$ ,  $C=K_D$ , k is sampling serial number,  $\Delta u(k)$  is the control increment, and e(k) is the input deviation value at the kth sampling time.  $K_P$  is scale factor,  $K_I$  is integral coefficient,  $K_I=K_P(T/T_1)$ , and  $K_D$  is differential coefficient,  $K_D=K_P(T_D/T)$ , T and  $T_D$  are sampling period and differential time, respectively.

A constant sampling period t was adopted in the computer control system. After determining  $K_P$ ,  $K_I$  and  $K_D$ , the control increment can be determined using Eq. (2) if the deviation of the three measurements is used. When an incremental algorithm is used, the control increment of the computer output  $\Delta u(k)$  corresponds to the increment of the actuator position, which can be determined as  $u(k)=u(k-1)+\Delta u(k)$ . The program framework of an incremental PID control algorithm is illustrated in Fig. 6. The detailed PID tuning process is described as follows.

(1) Application of incremental digital PID control algorithm in the isothermal extrusion process

For the simulation of the isothermal extrusion process, the change in the temperature of the extrudate at the die exit during the extrusion process was controlled by controlling the extrusion speed.

Equation (2) was applied to the isothermal extrusion simulation.  $T_0$  was set to be the highest

**Table 1** Contact boundary conditions in FE simulations

Boundary interface	Boundary type	Parameter definition	
Extrusion pad	In_flow	Extrusion speed: 5 mm/s; Extrusion pad temperature: 430 °C	
Cantainan	C-1: 111	Extrusion cylinder temperature: 430 °C; Friction type: purely stick;	
Container	Solid_wall	Heat transfer coefficient: 3000 W/(m <sup>2</sup> ·°C)	
Die	Solid_wall	Extrusion cylinder temperature: 430 °C; Friction type: purely stick;	
		Heat transfer coefficient: 3000 W/(m <sup>2</sup> .°C)	
Bearing	Bearing	Extrusion cylinder temperature: 430 °C; Friction type: shear friction;	
		Heat transfer coefficient: 3000 W/(m <sup>2</sup> .°C)	
Free surface	Free surface Free-surface Heat transfer coefficient with air: 20		
Outlet	Out_flow	Pressure: 0	

Table 2 Extrusion process parameters of 6063 aluminium alloy

Extrusion speed/(mm·s <sup>-1</sup> )	Billet temperature/°C	Porthole die temperature/°C	Container temperature/°C	Extrusion pad temperature/°C	Extrusion ratio
3-10	480	480	430	480	20

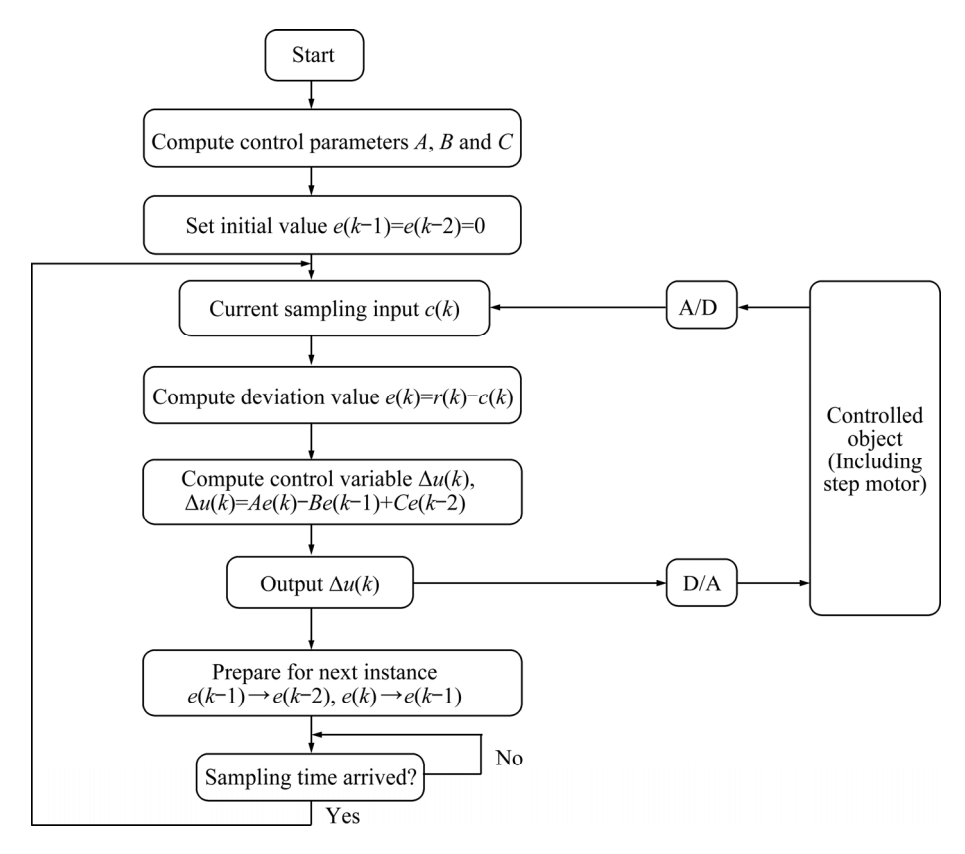


Fig. 6 Program block diagram of incremental PID control algorithm

target temperature of the extrusion, which was 530 °C in this simulation.  $T_k$ , which could be easily obtained from the FE simulation results, was the instantaneous maximum temperature of the extrudate during the kth sampling. The sampling period t was set as the ram displacement S, and  $e(k)=T_0-T_k$ . In accordance with Eq. (2),  $K_P$ ,  $K_I$ ,  $K_D$ and S must be determined. The control increment  $\Delta u(k)$  could be obtained by using the deviation between the previously obtained results and the results after three measurements. In the actual physical process, the output of a controller corresponds to the opening of an actuator. Therefore, the  $\Delta u(k)$  obtained through Eq. (2) in this simulation was assumed to be linearly related to the variation of the extrusion speed  $\Delta v$ . The assumption was  $\Delta v = \Delta u(k)/100$ . Therefore, in the next sampling period,  $v(k)=v(k-1)+\Delta v$ .

#### (2) PID control of isothermal extrusion process Given that the diameter of the blank was smaller than that of the extrusion barrel, the workpiece was in the upsetting process during the

first 25 steps of extrusion, and the extrusion rod was in the process of accelerating the metal material extrusion die orifice. The change in temperature

was small, and the target temperature was not reached. In addition, the control process was not added. After 25 steps, the billet material was extruded throughout the die orifice. During the extrusion process, severe plastic deformation caused a large amount of deformation heat, and the maximum temperature of the extrudate rapidly increased. The PID control was then executed at this time.

#### (3) Tuning of PID control parameters

In the PID control process, parameter  $K_P$  varies from 0 to 20, and the smaller the value is, the longer is the time for the temperature to reach the target temperature. However, when  $K_P$  is greater than 20, the temperature fluctuates obviously and cannot be controlled. On this basis, the integral adjustment was added. A certain value of  $K_P$  was adopted, and the value of  $K_I$  was increased (i.e. the effect of increasing integral). When  $K_I$  varies between 5 and 10, the static error can be eliminated, and the maximum temperature of a workpiece can be stabilized at the target temperature. When  $K_P$ =7 and  $K_I$ =7, the temperature control resulted in a fast response speed, the static error was eliminated, and a good isothermal control effect was achieved.

#### 5 Results and discussion

#### 5.1 Material flow behavior in porthole die

The material flow behavior during the entire extrusion process through the porthole die was analyzed. Figure 7 shows the flow behavior of the material at different stages of the porthole die. The colour depth and change reflected variations in flow velocity. The blue colour represents small velocity, whereas the red colour represents high velocity. The material flow velocity in contact with the container and porthole die surface is far lower than that at the die centre due to the strong adhesive friction. The difference between the maximum and minimum velocities of the material on the cross-section of the die exit is 5.02 mm/s, which indicates the uniform material flow velocity during the porthole extrusion process. The material supplies in different parts of the die cavity are reasonable, and the velocity distribution is relatively balanced. Therefore, the uniformity of temperature distribution on the cross-section of the extrudate is ensured.

## **5.2** Effect of extrusion speed on exit temperature rise and extrusion load

The transient FE models at seven extrusion speeds from 3 to 10 mm/s were established. After completing the simulation analysis, the average temperature of all nodes on the cross-section of the

profile 4 mm away from the die exit was extracted. In the first five steps of the extrusion process (ram displacement=25 mm), the extrusion ram was accelerated to extrude the billet through the porthole die. Consequently, the profile temperature rapidly increased. In this study, only the temperature change in the profile along the extrusion direction after 20 steps was considered.

Figure 8 shows the temperature variation of the profile during the transient extrusion process at an extrusion speed of 10 mm/s. When the billet is extruded by the porthole die, the heat change becomes a complex process that includes five components: (1) heat generation due to large plastic deformation, (2) heat generation due to the friction between the workpiece and the tools and dies (extrusion pad, container, and porthole die) and the local shear deformation in the dead metal zones, (3) heat energy conversion of the workpiece during the extrusion process, (4) heat conduction between the workpiece and the tools, and (5) heat exchange between the extrudate and the external environment (approximately 27 °C). Owing to the above heat changes, the temperature of the extrudate tends to increase during the extrusion process. temperature of the billet increases from 480 to 567.1 °C.

Figure 9 shows the temperature variation of the profile cross-section with the ram displacement at different extrusion speeds. With the increase in

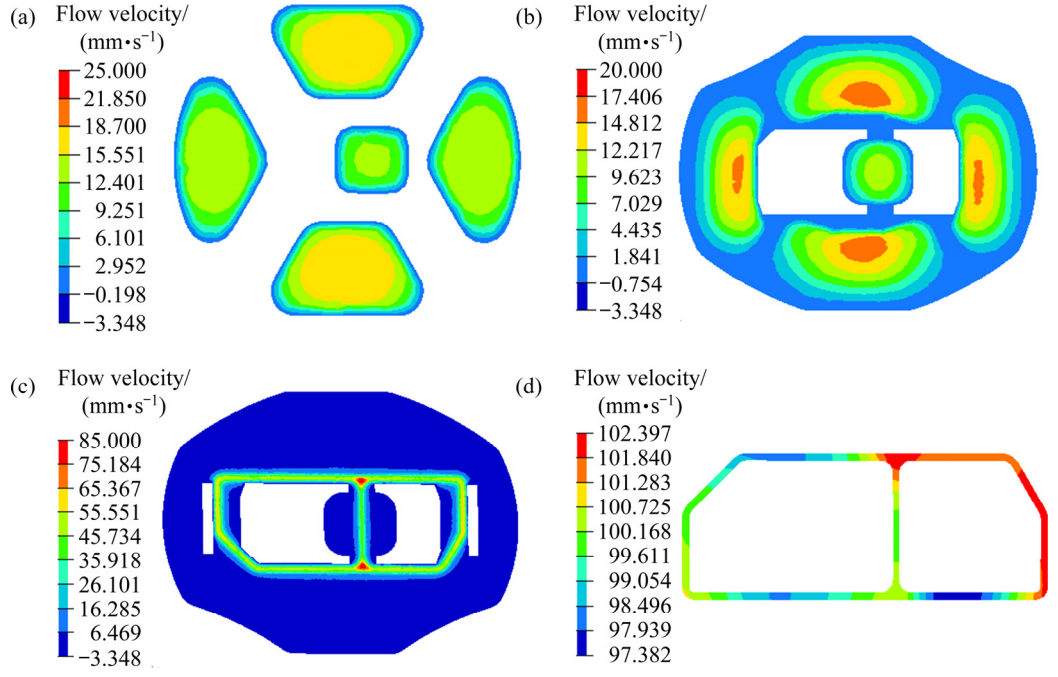
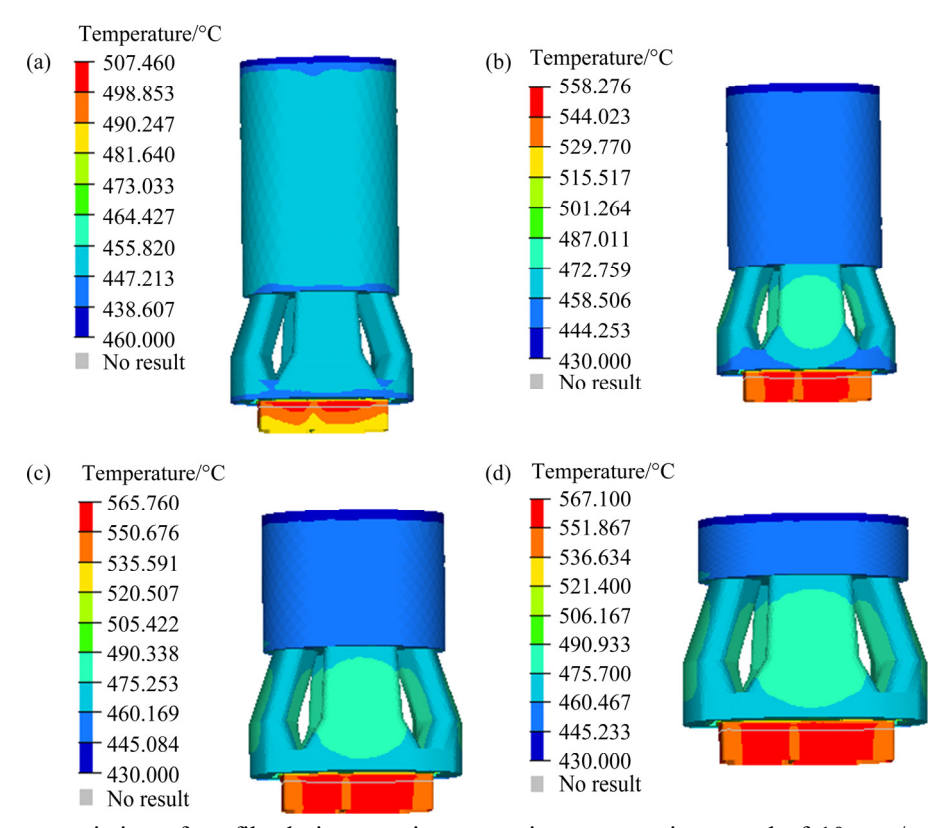


Fig. 7 Flow behavior of material at different stages in porthole die: (a) Entrance of porthole; (b) Welding stage; (c) Entrance of die orifice; (d) Die exit



**Fig. 8** Temperature variation of profile during transient extrusion at extrusion speed of 10 mm/s and different ram displacements: (a) S=20 mm; (b) S=85 mm; (c) S=160 mm; (d) S=250 mm

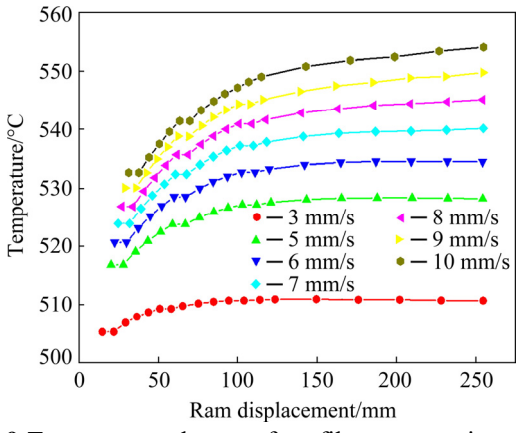


Fig. 9 Temperature change of profile cross-section at die exit with ram displacement after extrusion at different extrusion speeds

ram displacement, the average temperature of the profile cross-section at the die exit increases rapidly at first and then slows down. The reason for this phenomenon is that when the billet material is extruded into the die orifice, a strong local shear deformation will occur and a large amount of deformation heat that rapidly increases the temperature will be generated. As the extrusion process proceeds, the deformation heat transfers not only to the extrusion tools and the remaining billet,

but also to the extruded profile and external environment. Therefore, the exit temperature of the profile slowly increases before stabilizing. At an increased extrusion speed, the plastic deformation is severe, the plastic deformation heat increases and the average temperature of the cross-section at the die exit gradually rises. When the ram displacement is nearly 250 mm, the average temperature of the profile cross-section at the die exit at an extrusion speed of 3 mm/s is the lowest (510.7 °C). When the extrusion speed increases to 10 mm/s, the average temperature increases to 552 °C, which is 8.09% higher than that at 3 mm/s.

Figure 10 depicts the temperature difference of the profile cross-section along the extrudate length at different extrusion speeds. With the increase in extrusion speed, temperature difference along the extrudate length obviously increases. When the extrusion speed is 3 mm/s, temperature difference between the front and back ends of the extrudate is about 8 °C. When the extrusion speed increases to 7 mm/s, the temperature difference increases to 17.8 °C. When the extrusion further increases to 10 mm/s, the temperature difference rises to 21.4 °C. Such an increment is mainly related to the friction

between the billet and the porthole die, and the plastic deformation intensity of the billet and the dissipating heat time. At a slow extrusion speed, the heat conduction time between the billet and the extrusion tools is sufficient, and the friction heat generation between them is not obvious. In this case, the increase in the temperature of the billet is mainly caused by the heat transferred from the plastic deformation work. The increase in extrusion speed decreases the heat conduction time between the billet and the extrusion die. When the extrusion speed is high, almost no heat conduction will occur between the billet and porthole die. In addition, the friction between the billet and the die is high at a high extrusion speed, and thus results in a large amount of friction heat. These conditions lead to the gradual increase in the temperature variations of the profile along the extrudate length. The uneven temperature distribution along the extrudate length then leads to the non-uniformity of the microstructure and properties of a profile [9,10]. Therefore, controlling the temperature of a profile during the porthole die extrusion process is important.

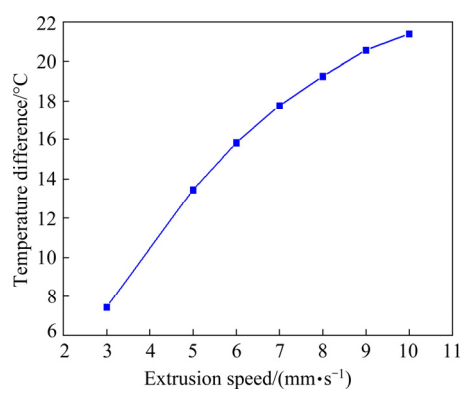


**Fig. 10** Temperature difference of profile cross-section along extrddate length at different extrusion speeds

Extrusion load has an important effect on die life, selection of extruder tonnage and production efficiency. Figure 11 shows the relationship between extrusion load and extrusion speed. With the increase in extrusion speed, the steady extrusion load gradually increases. The influence of extrusion speed on extrusion load is affected by many factors. The material deformation rate of a billet increases with the increase of extrusion speed. The increase in deformation rate then leads to a high critical shear stress and an effective stress in a material. Moreover, the deformation resistance of a material

increases with the increase of extrusion speed, whereas the plasticity of the material decreases. A deformed metal does not have sufficient time to recover and recrystallize. With the increase of extrusion speed, the deformation heat effect increases significantly. The generated heat during porthole die extrusion has no time to dissipate. As a result, the workpiece temperature increases, and the extrusion load is reduced. The steady extrusion load at an extrusion speed of 10 mm/s is 1450 t, which is far lower than the rated load of an extruder (1800 t). Therefore, a speed of 10 mm/s can be used as the maximum limit of the extrusion speed in the simulation of isothermal extrusion processes.

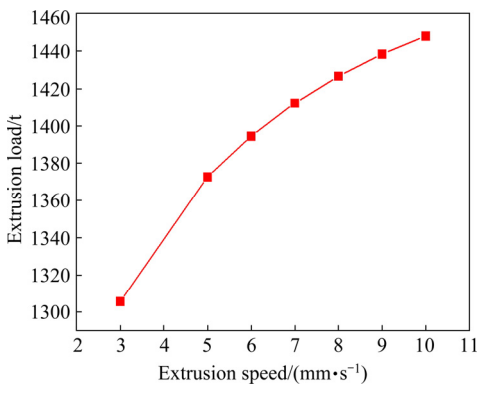


Fig. 11 Steady extrusion loads at different extrusion speeds

#### 5.3 Isothermal extrusion speed curve

The strengthening effect of an Al-Mg-Si alloy is mainly achieved through ageing precipitation. Increasing the degree of supersaturation increases the number of ageing precipitates, and therefore enhances the strengthening effect. Strengthening phase of Mg<sub>2</sub>Si solid solution can be produced in a matrix precipitate through solution quenching. The solid solution effect of Mg<sub>2</sub>Si phase and quenching effect can be enhanced by controlling the exit temperature between 520 °C and 550 °C during the extrusion process. In this study, the isothermal extrusion target temperature of the profile at the die exit was maintained at 530 °C, and the temperature difference of the profile cross-section along the extrudate length was controlled within 10 °C. To improve the extrusion efficiency, the initial extrusion speed was set to be a high value. However, because of the limitation of the actual extruder load, the extrusion speed should not be extremely large. A steady state cannot be achieved with a hydraulic control system at an extremely large extrusion speed. In consideration of the extrusion production efficiency, the minimum extrusion speed should be greater than 5 mm/s. Therefore, the variation range of extrusion speed was controlled at 5-10 mm/s. The PID control was used to control the average temperature of the profile cross-section at the die exit during the whole simulated extrusion process, and the obtained isothermal extrusion speed-stroke curve is shown in Fig. 12. At the beginning of the extrusion process, the initial speed will be set to be 10 mm/s when the PID control is not used. When the PID control is used, the extrusion speed will rapidly decrease to 6 mm/s when the ram displacement is 75 mm. The temperature stabilizes near the target temperature of 530 °C. As the extrusion process proceeds, the extrusion speed fluctuates, but the variations are small.

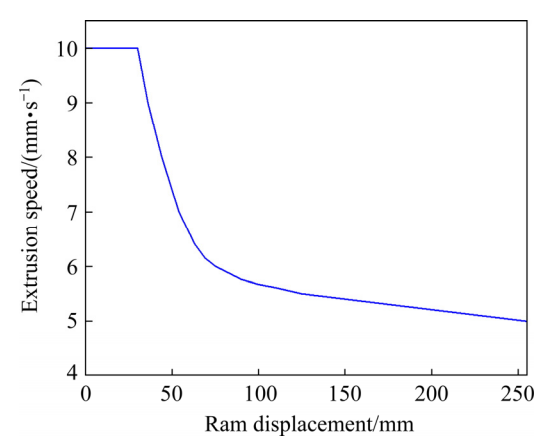
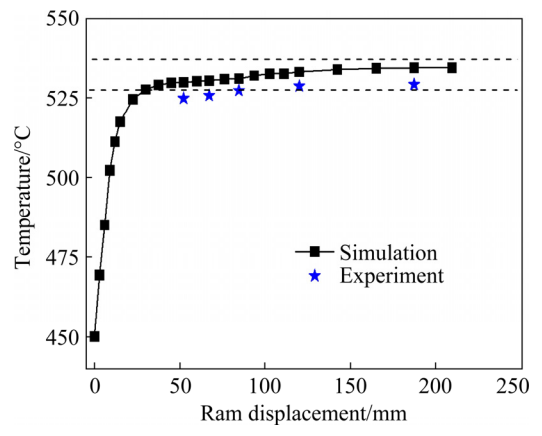


Fig. 12 Simulation of extrusion speed-stroke curve of isothermal extrusion

As previously mentioned, the temperature of the profile rapidly increases when the billet is extruded throughout the die orifice before reaching a stable value. The extrusion speed changes obviously at the early stage of extrusion, and the PID control process tracks the changes in the workpiece temperature. The extrusion speed slowly decreases until the extrusion process is complete. During the extrusion process, the extrusion speed decreases, and the deformation heat generated decreases through plastic deformation and friction. Meanwhile, the contact time and heat transfer from the workpiece to the extrusion tools increase. Therefore, the PID method implies that the heat generated by the plastic deformation, friction and the heat loss from the workpiece to the extrusion tools can be balanced by adjusting the extrusion speed.

### 5.4 Exit temperature during isothermal extrusion and experimental verification

Figure 13 shows the temperature variation of the profile at the die exit in variable speeds extrusion. The minimum temperature in the early stage of extrusion is 527.67 °C, whereas the maximum temperature in the late extrusion stage is 534.56 °C and the temperature difference between the front and back ends of the profile is about 6.9 °C. This result indicates that the establishment of the isothermal extrusion speed curve is accurate. When the extrusion speed curve is applied to the actual extrusion process, isothermal extrusion is realized. The accuracy and reliability of isothermal extrusion were verified using the PID algorithm and finite element simulation. An industrial non-contact infrared thermometer was used to monitor and record the temperature of the die exit. Figure 13 illustrates that the maximum error between the simulated and measured temperatures of the selected five positions is less than 8%. This result verifies the accuracy of the isothermal extrusion speed-stroke curve obtained using the PID algorithm.



**Fig. 13** Temperature change of die exit in variable speeds extrusion

#### **6 Conclusions**

- (1) As the ram displacement increased, the average temperature of the profile cross-section at the die exit increased rapidly and then slowly. When the ram displacement was approximately 250 mm, the average temperatures of the profile cross-section at the die exit at extrusion speeds of 3 and 10 mm/s were 510.7 and 552 °C, respectively.
- (2) The temperature difference of the profile cross-section along the extrudate length increased

with the increase in extrusion speed. When the extrusion speeds were 3 and 10 mm/s, the temperature differences between the front and back ends of profile at the die exit were about 8 °C and 21.4 °C, respectively.

- (3) The range of the extrusion speed was determined by considering the maximum extrusion load and production efficiency. By taking the optimal solution temperature of the secondary phase as the target temperature, the extrusion speed–stroke curve for realizing isothermal extrusion of the aluminium profile was obtained using an incremental PID control algorithm and FE simulations.
- (4) The exit temperature difference between the front and back ends of the extrudate along the extrusion direction obtained by adopting isothermal extrusion was about 6.9 °C. The heat generated by plastic deformation and friction during extrusion was balanced with the heat transfer from the workpiece to the container, porthole die and external environment.

#### Acknowledgments

The authors are grateful for the financial supports from the National Natural Science Foundation of China (No. 52005244), the Scientific Research Fund of Hunan Provincial Education Department, China (Nos. 18B285, 18B552), and the Natural Science Foundation of Hunan Provincial, China (Nos. 2019JJ50510, 2019JJ70077), and Young Scholars Program of Furong Scholar Program, China.

#### References

- REGGIANI B, DONATI L. Comparison of experimental methods to evaluate seam welds quality in extruded profiles
  Transactions of Nonferrous Metals Society of China, 2020, 30(3): 619–634.
- [2] XU X, ZHAO G Q, YU S B, WANG Y X, CHEN X X, ZHANG W D. Effects of extrusion parameters and post-heat treatments on microstructures and mechanical properties of extrusion weld seams in 2195 Al–Li alloy profiles [J]. Journal of Materials Research and Technology, 2020, 9(3): 2662–2678.
- [3] BAGHBANI BARENJI A, EIVANI A R, HASHE-MINIASARI M, JAFARIAN H R, PARK N. Effects of hot forming cold die quenching and inter-pass solution treatment on the evolution of microstructure and mechanical properties of AA2024 aluminum alloy after equal channel angular pressing [J]. Journal of Materials Research and Technology, 2020, 9(2): 1683–1697.

- [4] YI J, WANG G, LI S K, LIU Z W, GONG Y L. Effect of post-weld heat treatment on microstructure and mechanical properties of welded joints of 6061-T6 aluminum alloy [J]. Transactions of Nonferrous Metals Society of China, 2019, 29(10): 2035–2046.
- [5] LIU Z W, YI J, LI S K, NIE W J, LI L X, WANG G. Study on inhomogeneous cooling behavior of extruded profile with unequal and large thicknesses during quenching using thermo-mechanical coupling model [J]. Transactions of Nonferrous Metals Society of China, 2020, 30(5): 1211–1226.
- [6] LIU Z W, LI L X, WANG G, CHEN J R, YI J. Springback behaviors of extruded 6063 aluminum profile in subsequent multi-stage manufacturing processes [J]. International Journal of Advanced Manufacturing Technology, 2020, 109(1-2): 1-13.
- [7] ÖNDER A. A forming load analysis for extrusion process of AZ31 magnesium [J]. Transactions of Nonferrous Metals Society of China, 2019, 29(4): 741–753.
- [8] IKUMAPAYI O M, OYINBO S T, BODUNDE O P, AFOLALU SA, OKOKPUJIE I P, AKINLABI E T. The effects of lubricants on temperature distribution of 6063 aluminium alloy during backward cup extrusion process [J]. Journal of Materials Research and Technology, 2019, 8(1): 1175–1187.
- [9] LI L X, ZHOU J, DUSZCZYK J. Prediction of temperature evolution during the extrusion of 7075 aluminium alloy at various ram speeds by means of 3D FEM simulation [J]. Journal of Materials Processing Technology, 2004, 145(3): 360–370.
- [10] ZHANG C S, ZHAO G Q, CHEN Z R, CHEN H, KOU F J. Effect of extrusion stem speed on extrusion process for a hollow aluminum profile [J]. Materials Science and Engineering B, 2012, 177: 1691–1697.
- [11] YU J Q, ZHAO G Q, CUI W C, ZHANG C S, CHEN L. Microstructural evolution and mechanical properties of welding seams in aluminum alloy profiles extruded by a porthole die under different billet heating temperatures and extrusion speeds [J]. Journal of Materials Processing Technology, 2017, 247: 214–222.
- [12] BRYANT A J, DIXON W, FIELDING R A P, MACEY G. Isothermal extrusion [J]. Light Metal Age, 1999, 57(3):
- [13] BASTANI A F, AUKRUST T, BRANDAL S. Optimisation of flow balance and isothermal extrusion of aluminium using finite-element simulations [J]. Journal of Materials Processing Technology, 2011, 211(4): 650–667.
- [14] PENG Z, SHEPPARD T. A study on material flow in isothermal extrusion by FEM simulation [J]. Modelling and Simulation in Materials Science and Engineering, 2004, 12(5): 745.
- [15] ZHOU J, LI L X, DUSZCZYK J. 3D FEM simulation of the whole cycle of aluminium extrusion throughout the transient state and the steady state using the updated Lagrangian approach [J]. Journal of Materials Processing Technology, 2003, 134(3): 383–397.
- [16] QIAN D S, LI G C, DENG J D, WANG F. Effect of die structure on extrusion forming of thin-walled component with I-type longitudinal ribs [J]. International Journal of Advanced Manufacturing Technology, 2020, 108(5–6):

1959-1971.

- [17] BASTANI A F, AUKRUST T, BRANDAL S. Study of isothermal extrusion of aluminum using finite element simulations [J]. International Journal of Material Forming, 2010, 3(S1): 367–370.
- [18] VALDER G, TREEK J V. Billet heating options for isothermal extrusion [J]. Aluminium, 2016, 92(9): 24–28.
- [19] ZERBETTO M, FORZAN M, DUGHIERO F. Permanent magnet heater for a precise control of temperature in aluminum billets before extrusion [J]. Materials Today: Proceedings, 2015, 2(10): 4812–4819.
- [20] JENISTA D R. Extrusion billet taper quenching system [P]. US patent: US 5325694A, 1994–07–05.
- [21] LI Bo, ZHANG Nai-lu, ZHANG Ru. Simulated isothermal extrusion speed control system for titanium and titanium alloy profiles [J]. Information Recording Materials, 2019, 20(3): 7–9. (in Chinese)
- [22] LI Bo, ZHANG Nai-lu, ZHANG Ru. Simulated isothermal extrusion speed control system for titanium and titanium alloy profiles [J]. Information Recording Materials, 2019, 20(3): 7–9. (in Chinese)
- [23] PANDIT M, MÜLLER K. New measurement and automation system for extrusion plants [J]. Aluminium, 1999, 75(12): 1074–1076.
- [24] CHANDA T, ZHOU J, DUSZCZYK J. A comparative study on iso-speed extrusion and isothermal extrusion of 6061 Al alloy using 3D FEM simulation [J]. Journal of Materials Processing Technology, 2001, 114(2): 145–153.
- [25] YANG H, ZHANG J, HE Y M, HAN B T. Effect of temperature and ram speed on isothermal extrusion for large-size tube with piece-wing [J]. Journal of Materials Science & Technology, 2005, 21(4): 499–504.
- [26] LI L X, LOU Y. Ram speed profile design for isothermal extrusion of AZ31 magnesium alloy by using FEM simulation [J]. Transactions of Nonferrous Metals Society of China, 2008, 18(S1): 252–256.
- [27] ZHOU J, LI L X, DUSZCZYK J. Computer simulated and experimentally verified isothermal extrusion of 7075 aluminium through continuous ram speed variation [J].

- Journal of Materials Processing Technology, 2004, 146(2): 203-212.
- [28] TRUONG T T, HSU Q C, TONG V C. Effects of solid die types in complex and large-scale aluminum profile extrusion [J]. Applied Science, 2019, 10(1): 263.
- [29] CHEN L, LI Y Q, ZHAO G Q, ZHANG C S, GAO F Z. Multi- objective optimization and experimental investigation on hot extruded plate of high strength Al–Zn–Mg alloy [J]. Journal of Materials Research and Technology, 2020, 9(1): 507–519.
- [30] ZHAO Y, PEI J Y, GUO L L, YUN X B, MA H C. Effects of extrusion speed of continuous extrusion with double billets on welding performance of 6063 Al alloy [J]. Transactions of Nonferrous Metals Society of China, 2021, 31(6): 1561–1571.
- [31] LIU P, XIE S, CHENG L. Die structure optimization for a large, multi-cavity aluminum profile using numerical simulation and experiments [J]. Materials & Design, 2012, 36: 152–160.
- [32] LIU Z Z, LI L X, LI S K, YI J, WANG G. Simulation analysis of porthole die extrusion process and die structure modifications for an aluminum profile with high length-width ratio and small cavity [J]. Materials, 2018, 11(9): 1517.
- [33] NOSRATI A S, ABRINIA K. A new method for bearing design in the metal extrusion of profiled sections [J]. The International Journal of Advanced Manufacturing Technology, 2020, 106(3–4): 1069–1084.
- [34] SELLARS C M, TEGART W J M G. Hot workability [J]. International Materials Reviews, 1972, 17(1): 1–24.
- [35] LIU Z W, LI L X, WANG G, YI J. Analysis and improvement of material flow during extrusion process using spreading pocket die for large-size, flat-wide, and multi-ribs profile [J]. International Journal of Advanced Manufacturing Technology, 2020, 107(1–2): 4123–4138.
- [36] LI L X, ZHANG H, HU J, ZHOU J, DUSZCZYK J. Simulation-based design of ram speed profile for isothermal extrusion [J]. Key Engineering Materials, 2008, 367: 153-160.

### 基于 PID 算法和有限元模拟的 空心铝型材分流模等温挤压速度曲线设计

易 杰<sup>1</sup>, 刘志文<sup>2</sup>, 曾文琦<sup>1</sup>

1. 湖南工业职业技术学院 机械工程学院,长沙 410208; 2. 南华大学 机械工程学院,衡阳 421001

摘 要:利用增量式 PID 控制算法和有限元模拟相结合的方法,研究复杂空心铝型材的等温挤压过程。以最大挤压力和生产效率确定挤压速度范围。以二次相的较优固溶温度为目标温度,获得实现等温挤压的挤压速度-行程曲线。研究结果表明:在常规等速挤压过程中,随着挤压行程的增加,型材出模口横截面的平均温度先迅速升高后缓慢上升。随着挤压速度的增加,沿挤压方向的型材出模口温差增大。采用变化的挤压速度曲线,沿出模口挤压方向的前后温差约为 6.9 °C,挤压过程中塑性变形和摩擦所产生的热量与工件向挤压筒、分流模和外部环境传递的热量达到平衡。

关键词: 等温控制; 挤压速度曲线; 分流模挤压; PID 控制; 热量平衡